Published in final edited form as:
Sci Signal. 2011 September 27; 4(192): ra62. doi:10.1126/scisignal.2001630.

Akt determines cell fate through the negative regulation of the PERK-eIF2α phosphorylation pathway

Zineb Mounir[1,2], **Jothi Latha Krishnamoorthy**[1], **Shuo Wang**[1], **Barbara Papadopoulou**[3], **Shirley Campbell**[4], **William J. Muller**[4], **Maria Hatzoglou**[5], and **Antonis E. Koromilas**[1,6,*]

[1]Lady Davis Institute for Medical Research, Sir Mortimer B. Davis-Jewish General Hospital, Montreal, Quebec, H3T 1E2, Canada

[2]Division of Experimental Medicine, Faculty of Medicine, McGill University, Montreal, Quebec H3A 1A3, Canada

[3]Centre de Recherche en Infectiologie Centre Hospitalier de Québec, Pavillon CHUL, Québec, Canada

[4]Goodman Cancer Center, McGill University, Montreal, Quebec, Canada

[5]Departments of Nutrition, School of Medicine, Case Western University, Cleveland, Ohio 44106-4954, USA

[6]Department of Oncology, Faculty of Medicine, McGill University, Montreal, Quebec H2W 1S6, Canada

Abstract

Metazoans respond to various forms of environmental stress by inducing the phosphorylation of the α subunit of the translation initiation factor eIF2 at serine 51 (eIF2αP), a modification that leads to a global inhibition of mRNA translation. Herein, we demonstrate that eIF2αP is induced by pharmacological inhibition of the phosphoinositide-3-kinase (PI3K)-Akt pathway as well as by genetic or small interfering (si)RNA-mediated ablation of Akt. Increased eIF2αP is an evolutionary conserved process that involves the endoplasmic reticulum (ER)-resident protein kinase PERK, which is negatively regulated by Akt-dependent phosphorylation at threonine 799. PERK activity and eIF2αP are downregulated by activated Akt in mouse mammary gland tumors as well as in cells exposed to ER stress or oxidative stress leading to the induction of cell survival or death respectively. In unstressed cells, the PERK-eIF2αP pathway guards survival and facilitates adaptation to the deleterious effects of PI3K or Akt inactivation. As such, inactivation of the PERK-eIF2αP arm increases the susceptibility of tumor cells to death by pharmacological inhibitors of PI3K or Akt. Thus, in addition to mTOR the PERK-eIF2αP pathway provides a link between Akt signaling and translational control with implications in tumor formation and treatment.

Keywords

translational control; PERK; eIF2α phosphorylation; Akt/PKB; endoplasmic reticulum stress; oxidative stress; chemotherapeutic drugs

*Correspondence: Antonis E. Koromilas, PhD, Lady Davis Institute for Medical Research, Room 508, Sir Mortimer B. Davis-Jewish General Hospital, 3999 Cote Ste-Catherine Road, Montreal, Quebec H3T 1E2, Canada, Tel.: (514) 340 8222 local 3697; Fax: (514) 340 7576, antonis.koromilas@mcgill.ca.

Additional Methods and their associated references are included in the Supplementary Material.

Introduction

Control of mRNA translation is a crucial process in the regulation of expression of genes involved in cell growth, proliferation and differentiation [(1)]. Translational control is intimately involved in cancer development via the selective synthesis of proteins that influence tumor initiation, progression and metastasis [(2)]. Most of the regulation of mRNA translation is thought to be exerted at the initiation level through the coordinated action of several eukaryotic initiation factors (eIFs) that facilitate the recruitment of the ribosome to an mRNA and its positioning at the initiation codon [(3)]. Metazoans respond to various forms of environmental stress by blocking the initiation process via the induction of phosphorylation of the α subunit of eIF2 at serine 51 (S51) (herein referred to as eIF2αP) [(4)]. eIF2αP is mediated by a family of kinases each of which responds to distinct stimuli [(4)]. The family includes the heme-regulated inhibitor (HRI), whose activity is induced by heme deficiency and plays a role in regulation of globin synthesis; the general control non-derepressible-2 (GCN2), which is activated by uncharged t-RNA in response to amino acid deficiency; the endoplasmic reticulum (ER)-resident protein kinase PERK/PEK, whose activity is induced by the accumulation of unfolded proteins in the ER and represents as essential arm of the unfolded protein response (UPR); and the RNA-dependent protein kinase PKR, an interferon (IFN)-inducible protein activated by double-stranded (ds)RNA[(4)]. These enzymes exhibit significant sequence similarities, particularly in the protein kinase domain (KD), which explains their specificity towards eIF2α[(4)]. eIF2αP is implicated in tumorigenesis through its ability to act as either a promoter of cell survival or an inducer of cell death in response to various types of stress including DNA damage, oncogenic stress, ER stress or stress in tumor microenvironment [(5,6)].

Genetic alterations that lead to a gain in phosphoinositide-3-kinase (PI3K) signaling are commonly observed in human cancers[(7)]. Induction of PI3K activity following hormone, mitogen or growth factor stimulation results in the activation of Akt/protein kinase B (PKB), which phosphorylates several proteins involved in regulating cell survival and proliferation [(8)]. Among them, the mammalian target of rapamycin (mTOR) is a protein kinase which stimulates protein synthesis by mediating, directly or indirectly, the phosphorylation of proteins implicated in cap-dependent mRNA translation[(9)].

Our group recently demonstrated that eIF2αP by PKR mediates the pro-apoptotic properties of the tumor suppressor phosphatase and tensin homolog (PTEN) independently of PI3K-Akt signaling inhibition [(10)]. However, the possibility remains that the PI3K-Akt pathway signals to eIF2αP through a kinase other than PKR. Herein, we demonstrate that PERK acts downstream of Akt and promotes an adaptation process in response to PI3K-Akt pathway inhibition. We show that PERK is a substrate of Akt with important implications in the regulation of eIF2αP and Akt signaling in response to stress. We further show that inactivation of PERK and eIF2αP has profound effects on promoting tumor death in response to pharmacological inhibition of the PI3K-Akt pathway. As such, in addition to well-established role of the mTOR pathway the PERK-eIF2αP arm links Akt to translational control and affects Akt function in response to stress as well as the efficacy of tumor cell treatment with chemotherapeutic drugs targeting the PI3K-Akt pathway.

Results

Inhibition of PI3K induces eIF2αP and activates PERK

When human glioblastoma U87 cells, human breast cancer SkBr3 cells or spontaneously immortalized mouse embryonic fibroblasts (MEFs) were treated with the PI3K inhibitor LY294002, we observed an increase in eIF2αP at S51 in a time-dependent manner (Fig. 1A, figs. S1A, S1B). eIF2αP was also increased after treatment of U87 cells with GDC-0941,

which is a potent and specific inhibitor of PI3K [11] (Fig. 1B). Increased eIF2αP was specific for PI3K inhibitors because treatment of U87 cells with the mTOR inhibitor KU0063794 [12] or the MEK1 inhibitor PD98059 [13] did not affect eIF2αP (fig. S1C, S1D). Increased eIF2αP by PI3K inhibition is an evolutionary conserved process because it was also observed in *Drosophila melanogaster* embryo Kc167 cells after treatment with LY294002 (fig. S2A). The efficacy of LY294002 and GDC-0941 treatments in all cells was documented by the reduction of Akt phosphorylation at S473 as well as inhibition of GSK3β phosphorylation at S9 (Figs. 1A–B, fig. S1A, S1B). To identify the eIF2α kinase implicated in this process, we employed Kc167 cells to knockdown either dPERK or dGCN2, the two eIF2α kinases expressed in *Drosophila* cells, by siRNA. We noticed that siRNA-targeting of either dPERK (fig. S2B) or dGCN2 (fig. S2C) prevented the induction of deIF2αP by LY294002. Owing to the unavailability of antibodies for dPERK or dGCN2, we verified siRNA-mediated silencing by the lack of an induction of deIF2αP in Kc167 cells after treatment with inducers of each kinase such as thapsigargin (TG) (fig. S2B) and ultraviolet-C (UV-C) light (fig. S2C), which activate PERK [14] and GCN2 [15] respectively. These data implicated both dPERK and dGCN2 in eIF2αP in response to PI3K inhibition. To substantiate these observations in mammalian cells, we examined eIF2αP in MEFs lacking PERK and GCN2 (double knockout; DKO). We observed that unlike the wild-type (WT) MEFs, induction of eIF2αP was not possible in DKO MEFs after treatment with LY294002 (Fig. 1C). Additional experiments with MEFs lacking either PKR [16] or HRI [17] indicated that neither kinase is involved in eIF2αP by PI3K inhibition (fig. S3). This is further supported by our recent work demonstrating that PKR mediates eIF2αP downstream of PTEN independently of PI3K signaling inhibition [10]. Next, we looked at the phosphorylation of PERK at threonine (T) 980, an autophosphorylation site in the activation loop of the kinase that is essential for eIF2αP[14]. We found that LY294002 treatment of WT MEFs led to a substantial induction of PERK phosphorylation at T980, which was accompanied by an increase in eIF2αP (Fig. 1D). PERK activation was not due to an induction of ER stress because LY294002 treatment did not affect the splicing of X-box binding protein 1 (XBP-1) mRNA (fig. S4), which is as a reliable marker of UPR [18].

Inactivation of Akt leads to the induction of eIF2αP

To determine the mechanism of PERK activation, we employed *Drosophila* Kc167 cells to knock-down dAkt by siRNA. We found that dAkt downregulation increased the basal levels of deIF2αP, which, however, were not further increased after LY294002 treatment (fig. S5A). When WT MEFs and MEFs lacking Akt 1 and 2 (Akt DKO) [19] were used, we observed that Akt1,2-deficiency increased the basal levels of eIF2αP compared to WT MEFs (Fig. 2A, lanes 1, 4), which was further increased after elimination of the remainder Akt3 by siRNA (lane 7). We also observed that treatment with LY294002 induced eIF2αP at a higher level in WT MEFs than in Akt1,2 DKO MEFs treated with either scramble siRNA (control) or siRNA for Akt3 (Fig. 2A). This data indicated that Akt downregulation increases eIF2αP, which cannot be further increased by PI3K inhibition in Akt-deficient cells to the same extent as in Akt-proficient cells. To further support this data, we employed pharmacological inhibitors of Akt, such as inhibitor VIII and XI, both of which target the pleckstrin homology (PH) domain of Akt [20] or inhibitor IX, which directly inhibits Akt activity[20]. We observed that all inhibitors caused a substantial induction of eIF2αP in both mouse fibroblasts (Figs. 2B-D) and human tumor cells (figs. S5B–D). The efficiency of the treatments was verified by the impaired phosphorylation of Akt at S473 and ribosomal S6 protein at S235/236 (Figs. 2B–D; figs. S5B–D). Collectively, these data supported the notion that Akt has a negative effect on eIF2αP.

Akt inactivates PERK by phosphorylation at threonine 799

Mouse PERK contains seven serine and threonine residues all of which conform to a canonical RxRxxS/T phosphorylation consensus site for Akt (Fig. 3A). To test whether PERK is a substrate of Akt, we performed *in vitro* kinase assays using catalytically inactive GST-PERK and catalytically active Akt1 or Akt2. As control, we included GST-GSK3β in the assays, which is a bona-fide substrate of Akt. We found that active Akt induced the phosphorylation of GST-PERK as indicated in assays with radioactive ^{32}P-γATP (figs. S6A, B) or non-radioactive ATP after immunoblotting with phospho-Akt substrate-specific antibodies (fig. S6C). Phosphorylated GST-PERK was subsequently subjected to mass spectrometry, which identified phosphorylation at T799 only (Fig. 3B). T799 of mouse PERK and the surrounding consensus Akt substrate sequence are highly conserved in human and rat PERK (Fig. 3B). Transient transfection assays in COS-1 cells demonstrated the phosphorylation of Myc-PERK WT but not of Myc-PERK T799A after immunoprecipitation with Myc-antibodies and immunoblotting with phospho-Akt substrate-specific antibodies (Fig. 3C). Also, we noticed that T980 autophosphorylation of PERK, which is a marker of its activation, was more highly induced in Myc-PERK T799A than in Myc-PERK WT after expression in Cos-1 cells with Myc-Akt1 (Fig. 3D). Furthermore, Cos-1 cells expressing Myc-PERK T799A displayed a higher level of endogenous eIF2αP than cells expressing Myc-PERK WT consistent with the increased autophosphorylation capacity of Myc-PERK T799A at T980 (Fig. 3D). These data demonstrated that T799 phosphorylation plays a negative role in PERK activation.

Akt antagonizes the PERK-eIF2αP pathway in stressed and tumor cells

The PERK-eIF2αP arm is an important element of the switch from the pro-survival to pro-death signaling during chronic or severe ER stress leading to the induction of the activating transcription factor 4 (ATF4) and CCAAT/enhancer binding protein (C/EBP) homologous protein (CHOP) [21,22]. On the other hand, activation of Akt in ER-stressed cells has been largely associated with cell survival [23,24]. As such, we wished to examine the possible connection between PERK and Akt in response to ER stress. When WT and isogenic Akt DKO MEFs [19] were treated with TG, we observed that Akt promoted cell survival in response to ER stress (Fig. 4A). However, PERK phosphorylation at T980 and eIF2αP were more highly induced in DKO than in WT MEFs after TG treatment (Fig. 4B). Also, the ability of Akt to impair the induction of eIF2αP under ER stress was also observed in human HT1080 cells in which all three Akt isoforms were ablated by siRNA (fig. S7). Moreover, Akt-mediated phosphorylation of PERK was impaired in Akt DKO MEFs compared to WT MEFs after treatment with TG (Fig. 4C). Taken together, these data suggested that Akt negatively regulates PERK by phosphorylation at T799 in response to ER stress. We further observed that the higher levels of PERK activity and eIF2αP in Akt DKO MEFs were associated with increased ATF4 and CHOP expression indicating that the higher susceptibility of the DKO MEFs to cell death by ER stress may be mediated, at least in part, by the activation of the ATF4-CHOP arm (Fig. 4B). The pro-apoptotic role of PERK was confirmed in experiments showing that blockade of endogenous PERK by the expression of the dominant-negative and catalytically inactive Myc-PERK K618A caused a 40% decrease in the susceptibility of Akt DKO MEFs to death in response to ER stress (Fig. 4D). Collectively, these data demonstrated that Akt-mediated phosphorylation of PERK prevents the induction of apoptosis under prolonged ER stress.

Contrary to its function in ER stress, Akt plays a pro-apoptotic role in cells subjected to oxidative stress [25]. Consistent with previous studies [25], we observed a higher susceptibility of WT MEFs than Akt DKO MEFs to death after treatment with H_2O_2 (Fig. 5A). We also saw that H_2O_2 treatment resulted in a higher induction of eIF2αP and PERK phosphorylation at T980 in Akt DKO MEFs than in WT MEFs (Fig. 5B). Similarly, eIF2αP

was more highly induced in human HT1080 cells in which all three Akt isoforms were targeted by siRNA than in cells with intact Akt after exposure to H_2O_2 (fig. S7). We further noticed that Akt-mediated phosphorylation of PERK was impaired in DKO MEFs compared to WT MEFs exposed to H_2O_2 (Fig. 5C). These data demonstrated that Akt activation results in the inhibition of PERK-eIF2αP arm in cells under oxidative stress. To address the biological role of Akt-mediated phosphorylation of PERK, $PERK^{-/-}$ MEFs were reconstituted with either Myc-PERK WT or Myc-PERK T799A followed by treatment with H_2O_2. We observed that the pro-apoptotic effects of H_2O_2 were reduced by 50% in $PERK^{-/-}$ cells reconstituted with PERK T799A compared to mock transfected cells or cells reconstituted with PERK WT (Fig. 5D). These data confirmed that PERK inactivation by phosphorylation at T799 promotes the pro-apoptotic effects of Akt in cells subjected to oxidative stress. Thus, PERK antagonizes Akt-mediated cell death in response to oxidative stress.

We further examined whether inactivation of the PERK-eIF2αP arm by Akt can be observed *in vivo*. To this end, we employed transgenic mice expressing a constitutively active form of Akt1 (Akt1-DD) together with an oncogenic version of ErbB2/Neu (NDL) under the control of the mammary tumor virus (MMTV) promoter [(26)]. Expression of Akt1-DD in NDL mice significantly accelerates mammary gland tumor progression compared to NDL mice alone [(26)]. When mammary tumors from these transgenic mice were used, we observed that NDL tumors contained increased levels of PERK activity, which were detected by immunohistochemical (IHC) analysis of PERK phosphorylated at T980, as opposed to NDL tumors expressing Akt1-DD, in which detection of PERK activity by IHC was not possible (Fig. 6). We also looked at PERK activity and eIF2αP in tumor samples by immunoblotting, and we observed that NDL tumors contained both increased levels of PERK phosphorylation at T980 and eIF2αP compared to NDL tumors expressing Akt1-DD (Fig. 6). The activity of Akt1-DD in tumors was indicated by the increased levels of Akt phosphorylated at S473 as became evident by IHC analysis as well as immunoblotting (Fig. 6). These data demonstrated the inhibition of the PERK-eIF2αP pathway by activated Akt *in vivo*.

eIF2αP is an adaptive response to PI3K and Akt inhibition with implications in cancer treatment

To further address the significance of our findings, we investigated the biological role of eIF2αP in response to PI3K-Akt pathway inhibition. To this end, we employed MEFs bearing a S51A knock-in homozygous mutation of eIF2α (i.e. eIF2αA/A MEFs) together with their isogenic WT counterparts (i.e. eIF2αS/S MEFs) [(27)]. We observed that treatment of both MEF types with LY294002 increased G_0/G_1 arrest and induced apoptosis, effects that were more prominent in eIF2αA/A than in eIF2αS/S MEFs (Fig. 7A, fig. S8A). In line with these findings, treatment of the MEFs with the Akt inhibitor VIII, IX or XI resulted in a higher induction of death in eIF2αA/A MEFs than in eIF2αS/S MEFs as documented by flow cytometry analysis (Fig. 7B–C, fig. S8B). Collectively, these data demonstrated that eIF2αP promotes cell survival in response to PI3K-Akt pathway disruption. They also implied that elimination of the cytoprotective effects of eIF2αP could render tumor cells more susceptible to death after treatment with drug inhibitors of the PI3K-Akt pathway. To address this possibility, we used HT1080 fibrosarcoma cells to target PERK by siRNA as demonstrated by the decreased levels of PERK expression and impaired induction of eIF2αP after treatment with PI3K and Akt inhibitors (fig. S9). We observed that treatment with either the PI3K inhibitor GDC-0941 or Akt inhibitor XI induced cell death more efficiently in cells with inactivated PERK than in cells with intact PERK (Figs. 7D, E). These findings demonstrated that elimination of the cytoprotective effects of the PERK-

eIF2αP arm can render tumor cells more susceptible to death after treatment with drug inhibitors of the PI3K-Akt pathway.

Discussion

Our study reveals an essential role of Akt signaling in the negative regulation of eIF2αP. Although genetic analysis implicates both PERK and GCN2 in this process, it is not presently known how GCN2 activity is controlled by Akt. A previous study in budding yeast indicated an indirect role of TOR in the regulation of GCN2, the only eIF2α kinase in this organism. That is, TOR inhibition by rapamycin induced the dephosphorylation of GCN2 at S577, a modification that leads to GCN2 activation and induction of eIF2αP [(28)]. However, S577 is not conserved in other GCN2 orthologs [(28)] suggesting that negative regulation of GCN2 by mTOR is not a universal mechanism. Consistent with this notion, pharmacological inhibition of mTOR did not affect eIF2αP in U87 cells (fig. S1C) indicating that mammalian GCN2 is controlled by the PI3K-Akt pathway at a level different from mTOR. Nevertheless, our biochemical and biological data clearly demonstrate an important role of PERK in the induction of eIF2αP in response to PI3K and/or Akt inhibition. Our study further demonstrates that the ability of Akt to function as a "check point" of survival or death is affected by the inactivation of PERK by phosphorylation at T799 (see model fig. S10).

The biological implications of our findings are highlighted by the ability of PERK and Akt to respond to ER stress and oxidative stress, two forms of stress that are intimately linked to tumorigenesis. Specifically, ER stress is induced in solid tumors deprived from nutrients, glucose and oxygen as a result of limited tumor vascularization [(29,30)]. Under these conditions, tumor cells have developed mechanisms to adapt to ER stress in order to maintain their survival and growth. Mild forms of ER stress in tumors leads to PERK activation, which promotes adaptation through translational and transcriptional mechanisms [(29)]. However, tumor adaptation becomes faulty under conditions of severe or chronic forms of ER stress [(21,22)] leading to the induction of a pro-apoptotic program that is orchestrated not only by the sustained activation of PERK (Fig. 4) but also by the inactivation of Akt [(31)]. Cell adaptation through PERK and eIF2αP also involves inhibition of ROS production and reduction of damage caused from oxidative stress as part of an anti-oxidant mechanism that utilizes the induction of ATF4 [(32,33)] and expression of NF-E2-related factor 2 (Nrf2) [(34)]. The anti-oxidant function of PERK has profound effects on tumor promotion [(35,36)] as well as tumor resistance to chemotherapeutic drugs [(36)]. Contrary to PERK and eIF2αP, Akt increases ROS synthesis through the inhibition of the transcriptional function of FoxO proteins [(25)]. Akt may further increase ROS synthesis by downregulating the PERK-eIF2αP arm, which in turn facilitates cell death from oxidative stress (Fig. 5 and Ref. [(25)]). The ability of Akt to respond to oxidative stress has also been linked to the induction of senescence in mouse and human fibroblasts [(25,37)]. The pro-senescent function of Akt may have implications not only in the regulation of tumorigenesis but also in the development of metabolic diseases such as insulin resistance and diabetes [(38)]. Unlike Akt, the role of PERK in regulation of senescence is not known although eIF2αP has been shown to be increased in senescent cells as part of UPR [(39,40)]. Several observations support the notion that UPR is compromised with aging [(41)] indicating that PERK and eIF2αP may play a role in senescence initiated by activated Akt.

Our study provides evidence for a role of PERK and eIF2αP in anti-cancer therapies targeting the PI3K pathway. Specifically, we show that the ability of activated Akt to impair the PERK-eIF2αP arm is a property of tumor cells grown *in vitro* as well as *in vivo* (Fig. 6). We also show that inactivation of the cytoprotective effects of the PERK-eIF2αP arm increases the susceptibility of human tumor cells to death by inhibitors of PI3K or Akt (Fig. 7). This is consistent with many studies showing that drug inhibitors of PI3K and Akt

signaling are inducers of apoptosis in several types of cancer; however, the best use of them in the clinics is in combination with other chemotherapies [42]. Our data show that inactivation of PERK and eIF2αP may be a suitable means to improve the efficacy of current chemotherapies targeting PI3K-Akt signaling. Our data suggest that eIF2αP may represent an important mechanism of addiction of tumor cells to chemotherapeutic drugsand as such, it is a potential target for anti-cancer therapy.

Materials and Methods

Plasmids

Myc-PERK wild type, Myc-PERK K618A and GST-PERK K618A constructs were described elsewhere [14].

Cell culture and treatments

$PKR^{-/-}$, $PERK^{-/-}$ or $HRI^{-/-}$ MEFs and their isogenic wild type counterparts were maintained in culture as described [43]. eIF2α S/S and eIF2α A/A MEFs were cultured as described elsewhere [27]. The culture of Akt DKO MEFs and their isogenic wild type MEFs was described elsewhere [25]. HT1080 and U87 cells were cultured as previously described [10,44]. *Drosophila* Kc167 cells were obtained from Drosophila Genomics Resource Center (DGRC) and were grown in Shields and Sang insect medium containing yeast extract (1g/L), bactopeptone (2.5g/L) and 5% heat-inactivated fetal calf serum. The MCF-7 cells were maintained in RPMI-1640 media supplemented with 10% heat-inactivated calf serum. LY294002 (Biomol), H_2O_2 (Biorad), bortezomib (LC laboratories), thapsigargin (Sigma), the Akt inhibitors VIII, IX or XI (EMD Chemicals), GDC-0941 (Selleck Chemicals), PD98059 (Selleck Chemicals) and KU0063794 (Bethyl laboratories) were used in concentrations described in figure legends. Treatments with LY294002 were refreshed every 12 hours up to indicated time points of the experiments.

Protein extraction, immunoblotting and immunoprecipitation

Protein extraction from mouse and human cells was performed as described [10]. Protein extraction from *Drosophila* Kc167 cells was performed as described [45]. Immunoblot analyses of protein extracts was performed as described [10]. The primary antibodies were as follows: anti-dAkt pS505 rabbit polyclonal antibody (Cell Signaling), anti-Akt/PKB pS473 rabbit polyclonal antibody (Cell Signaling), anti-Akt/PKB rabbit polyclonal antibody (Cell Signaling), anti-S6-pSer235/236 rabbit polyclonal antibody (Cell Signaling), rabbit serum to phospho-S51 of eIF2α (Invitrogen), anti-eIF2α rabbit polyclonal antibody (Santa Cruz), anti-Myc antibody (Santa Cruz), anti-actin mouse monoclonal antibody (ICN), anti-PKR (B10) mouse monoclonal antibody (Santa Cruz), anti-PERK pT980 rabbit monoclonal antibody (Cell Signaling), homemade anti-PERK mouse monoclonal antibody, anti-phospho S/T Akt substrate antibody (Cell Signaling), anti-ATF4 antibody (Proteintech group), anti-CHOP antibody (Santa Cruz). The secondary antibodies were horseradish peroxidase (HRP)-conjugated anti-mouse IgG antibody and HRP-conjugated anti-rabbit IgG antibody (Amersham Pharmacia Biotech). Myc-tagged proteins were immunoprecipitated from 500 μg protein extracts using 2 μg of anti-Myc antibody conjugated to anti-mouse IgG sepharose beads (Sigma). Endogenous PERK was immunoprecipitated from 500 μg protein extracts using 5 μg homemade anti-PERK monoclonal antibody coupled to anti-mouse IgG sepharose beads (Sigma).

DNA transfections

Transient transfections of COS1 cells were performed using Lipofectamine Plus Reagent (Invitrogen) following the manufacturer's protocol. Cells (5×10^5) were seeded in 60mm

plates and 5 μg of plasmid DNA was used for transfection. Cells were then incubated at 37°C for 48hrs including any treatment.

RNA interference

MEFs were transfected with siRNA using the *Amaxa Nucleofector* system (MEF kit 1) according to manufacturer's specifications. HT1080 cells were transfected with siRNA using LipoFectamine 2000 according to manufacturer's specifications. Treatment of cells with siRNA against mouse Akt3 (SMARTpool, Dharmacon), human Akt1, Akt2 and Akt3 (SMARTpool, Dharmacon), human PERK (SMARTpool, Dharmacon) or scrambled control siRNA (Dharmacon) was performed for 48hrs.

Drosophila RNAi and analysis

dsRNAs for targeting *Drosophila* Akt/PKB, S6K, PERK and GCN2 were synthesized by *in vitro* transcription in 20μl reactions using a T7 MEGAscript™ RNAi kit (Ambion). DNA templates for IVT were generated by RT-PCR from total *Drosophila* cellular RNA using the TRIzol reagent as specified by the manufacturer (Invitrogen). As silencing control human transferrin receptor dsRNA (TfR) was generated by RT-PCR from total RNA obtained from human HT1080 cells. Primers (which incorporated a 5′ and 3′ T7 promoter) for dAkt/dPKB, dS6K, dPERK and dGCN2 dsRNA synthesis are listed in the supplemental material. *Drosophila* Kc167 cells (1×10^6) were diluted in 1ml serum-free medium and incubated with dsRNA (20μg) in a six-well cell culture dish for 30min at room temperature followed by addition of 2ml of media containing 10% fetal bovine serum. The cells were incubated for additional 3 days to allow turnover of the target protein.

Flow cytometry analysis

Cells were seeded (2×10^5 cells) in 100 mm plates and treated with LY294002, thapsigargin, H_2O_2 or Akt inhibitors VIII, IX or XI at the concentrations and times indicated in the text. Cells were detached with phosphate buffer saline (PBS) that contained 1mM EDTA and centrifuged at 900xg for 5 minutes. Cells were fixed by adding 4 ml of ice-cold 70% ethanol gently to the pellet and stored at −20°C overnight. For staining, ethanol was removed and cells were re-suspended in 0.5 ml of PBS containing 50 μg/ml propidium iodide (P4170, Sigma) and 20 μg/ml RNase (Sigma). Cells were incubated at room temperature for 30 minutes in the dark and subjected to flow cytometry analysis on a FACScan cell sorter. PERK $^{-/-}$ MEFs and Akt1 $^{-/-}$ Akt2 $^{-/-}$ DKO MEFs were transfected with pcDNA-GFP plasmid alone or together with plasmid DNA bearing either Myc-PERK wild-type cDNA, Myc-PERK T799A cDNA or Myc-PERK K618A cDNA. Forty eight hours after transfection, cells were treated with H_2O_2 (0.5mM) for 2 and 4 hours or thapsigargin (1μM) for 18 and 24 hours. The GFP-positive cells were gated and their subG_1 levels analyzed by FACS following staining with Hoechst 33342 (10 μg/ml).

In vitro phosphorylation assays

In vitro Akt kinase assays with GST-PERK K618A and GST-GSK3β K85R/K86R as substrate were performed using ^{32}P-γATP, 25mM MgAc and 0.25mM cold ATP. For Akt1 (Upstate), kinase reaction buffer contained 40mM MOPS/NaOH and 1mM EDTA; for Akt1 (Biomol), 25mM MOPS, 12.5mM β-glycerophosphate, 5mM EGTA, 2mM EDTA, 25mM $MgCl_2$, 0.25mM DTT; for GST-Akt2 (Biomol), 50mM Tris, 0.5mM DTT, 1mM EGTA, 0.2mM sodium orthovanadate. Kinase reactions were incubated for 30min at 30°C. Samples were subjected to SDS-PAGE, stained with Coomassie blue and subjected to autoradiography. Non-radioactive *in vitro* Akt kinase assays were performed as described above in the presence of 3 mM ATP. The mass spectrometry procedure is included in the supplementary materials.

Statistical analysis

All quantitative variables are presented as means ± S.D. We compared the differences of three groups or more using one-way ANOVA and the differences of two groups using two-tailed Student *t* test (GraphPad Prism 5), and $p < 0.05$ was considered statistically significant.

Supplementary Material

Refer to Web version on PubMed Central for supplementary material.

Acknowledgments

We thank D. Ron for Myc-tagged and GST-tagged PERK constructs as well as for PERK$^{-/-}$ and PERK$^{-/-}$ GCN2$^{-/-}$ MEFs; R. J. Kaufman for HRI$^{+/+}$ and HRI$^{-/-}$ MEFs as well as eIF2αS/S and eIF2αA/A MEFs; N. Hay for WT and Akt1$^{-/-}$ Akt2$^{-/-}$ MEFs; P.N. Tsichlis for Myc-Akt1 plasmid; N. Benlimame for IHC analysis of the mouse tissues; Koromilas lab members for helpful discussions. Mass spectrometry analysis was performed by the Proteomics platform of the Eastern Quebec Genomics Center, Quebec, Canada. IHC analysis was performed at the Georges and Olga Minarik Research Pathology Facility at the Segal Cancer Centre, Jewish General Hospital, Montreal, Canada. The work is supported by MOP-38160 grant from the Canadian Institutes of Health Research (CIHR) and a grant from the Quebec Breast Cancer Foundation (QBCF) to AEK as well as the DK60596 and DK53307 grants from the National Institutes of Health (NIH) to MH. ZM is the recipient of a Canada Graduate Studentship Doctoral Award from CIHR.

References and Notes

1. Holcik M, Sonenberg N. Translational control in stress and apoptosis. Nat Rev Mol Cell Biol. 2005; 6:318–327. [PubMed: 15803138]
2. Silvera D, Formenti SC, Schneider RJ. Translational control in cancer. Nat Rev Cancer. 2010; 10:254–266. [PubMed: 20332778]
3. Sonenberg N, Hinnebusch AG. Regulation of translation initiation in eukaryotes: mechanisms and biological targets. Cell. 2009; 136:731–745. [PubMed: 19239892]
4. Wek RC, Jiang HY, Anthony TG. Coping with stress: eIF2 kinases and translational control. Biochem Soc Trans. 2006; 34:7–11. [PubMed: 16246168]
5. Raven JF, Koromilas AE. PERK and PKR: old kinases learn new tricks. Cell Cycle. 2008; 7:1146–1150. [PubMed: 18418049]
6. Wouters BG, Koritzinsky M. Hypoxia signalling through mTOR and the unfolded protein response in cancer. Nat Rev Cancer. 2008; 8:851–864. [PubMed: 18846101]
7. Liu P, Cheng H, Roberts TM, Zhao JJ. Targeting the phosphoinositide 3-kinase pathway in cancer. Nat Rev Drug Discov. 2009; 8:627–644. [PubMed: 19644473]
8. Manning BD, Cantley LC. AKT/PKB signaling: navigating downstream. Cell. 2007; 129:1261–1274. [PubMed: 17604717]
9. Ma XM, Blenis J. Molecular mechanisms of mTOR-mediated translational control. Nat Rev Mol Cell Biol. 2009; 10:307–318. [PubMed: 19339977]
10. Mounir Z, Krishnamoorthy JL, Robertson GP, Scheuner D, Kaufman RJ, Georgescu MM, Koromilas AE. Tumor suppression by PTEN requires the activation of the PKR-eIF2alpha phosphorylation pathway. Sci Signal. 2009; 2:ra85. [PubMed: 20029030]
11. Folkes AJ, Ahmadi K, Alderton WK, Alix S, Baker SJ, Box G, Chuckowree IS, Clarke PA, Depledge P, Eccles SA, Friedman LS, Hayes A, Hancox TC, Kugendradas A, Lensun L, Moore P, Olivero AG, Pang J, Patel S, Pergl-Wilson GH, Raynaud FI, Robson A, Saghir N, Salphati L, Sohal S, Ultsch MH, Valenti M, Wallweber HJ, Wan NC, Wiesmann C, Workman P, Zhyvoloup A, Zvelebil MJ, Shuttleworth SJ. The identification of 2-(1H-indazol-4-yl)-6-(4-methanesulfonyl-piperazin-1-ylmethyl)-4-morpholin-4-yl-t hieno[3,2-d]pyrimidine (GDC-0941) as a potent, selective, orally bioavailable inhibitor of class I PI3 kinase for the treatment of cancer. J Med Chem. 2008; 51:5522–5532. [PubMed: 18754654]

12. Garcia-Martinez JM, Moran J, Clarke RG, Gray A, Cosulich SC, Chresta CM, Alessi DR. Ku-0063794 is a specific inhibitor of the mammalian target of rapamycin (mTOR). Biochem J. 2009; 421:29–42. [PubMed: 19402821]

13. Dudley DT, Pang L, Decker SJ, Bridges AJ, Saltiel AR. A synthetic inhibitor of the mitogen-activated protein kinase cascade. Proc Natl Acad Sci USA. 1995; 92:7686–7689. [PubMed: 7644477]

14. Harding HP, Zhang Y, Ron D. Protein translation and folding are coupled by an endoplasmic-reticulum-resident kinase. Nature. 1999; 397:271–274. [PubMed: 9930704]

15. Deng J, Harding HP, Raught B, Gingras AC, Berlanga JJ, Scheuner D, Kaufman RJ, Ron D, Sonenberg N. Activation of GCN2 in UV-irradiated cells inhibits translation. Curr Biol. 2002; 12:1279–1286. [PubMed: 12176355]

16. Abraham N, Stojdl DF, Duncan PI, Methot N, Ishii T, Dube M, Vanderhyden BC, Atkins HL, Gray DA, McBurney MW, Koromilas AE, Brown EG, Sonenberg N, Bell JC. Characterization of transgenic mice with targeted disruption of the catalytic domain of the double-stranded RNA-dependent protein kinase, PKR. J Biol Chem. 1999; 274:5953–5962. [PubMed: 10026221]

17. Han AP, Yu C, Lu L, Fujiwara Y, Browne C, Chin G, Fleming M, Leboulch P, Orkin SH, Chen JJ. Heme-regulated eIF2alpha kinase (HRI) is required for translational regulation and survival of erythroid precursors in iron deficiency. EMBO J. 2001; 20:6909–6918. [PubMed: 11726526]

18. Calfon M, Zeng H, Urano F, Till JH, Hubbard SR, Harding HP, Clark SG, Ron D. IRE1 couples endoplasmic reticulum load to secretory capacity by processing the XBP-1 mRNA. Nature. 2002; 415:92–96. [PubMed: 11780124]

19. Peng XD, Xu PZ, Chen ML, Hahn-Windgassen A, Skeen J, Jacobs J, Sundararajan D, Chen WS, Crawford SE, Coleman KG, Hay N. Dwarfism, impaired skin development, skeletal muscle atrophy, delayed bone development, and impeded adipogenesis in mice lacking Akt1 and Akt2. Genes Dev. 2003; 17:1352–1365. [PubMed: 12782654]

20. Lindsley CW, Barnett SF, Layton ME, Bilodeau MT. The PI3K/Akt pathway: recent progress in the development of ATP-competitive and allosteric Akt kinase inhibitors. Curr Cancer Drug Targets. 2008; 8:7–18. [PubMed: 18288939]

21. Ron D, Walter P. Signal integration in the endoplasmic reticulum unfolded protein response. Nat Rev Mol Cell Biol. 2007; 8:519–529. [PubMed: 17565364]

22. Szegezdi E, Logue SE, Gorman AM, Samali A. Mediators of endoplasmic reticulum stress-induced apoptosis. EMBO Rep. 2006; 7:880–885. [PubMed: 16953201]

23. Hu P, Han Z, Couvillon AD, Exton JH. Critical role of endogenous Akt/IAPs and MEK1/ERK pathways in counteracting endoplasmic reticulum stress-induced cell death. J Biol Chem. 2004; 279:49420–49429. [PubMed: 15339911]

24. Hosoi T, Hyoda K, Okuma Y, Nomura Y, Ozawa K. Akt up- and down-regulation in response to endoplasmic reticulum stress. Brain Res. 2007; 1152:27–31. [PubMed: 17434462]

25. Nogueira V, Park Y, Chen CC, Xu PZ, Chen ML, Tonic I, Unterman T, Hay N. Akt determines replicative senescence and oxidative or oncogenic premature senescence and sensitizes cells to oxidative apoptosis. Cancer Cell. 2008; 14:458–470. [PubMed: 19061837]

26. Hutchinson JN, Jin J, Cardiff RD, Woodgett JR, Muller WJ. Activation of Akt-1 (PKB-alpha) can accelerate ErbB-2-mediated mammary tumorigenesis but suppresses tumor invasion. Cancer Res. 2004; 64:3171–3178. [PubMed: 15126356]

27. Scheuner D, Song B, McEwen E, Liu C, Laybutt R, Gillespie P, Saunders T, Bonner-Weir S, Kaufman RJ. Translational control is required for the unfolded protein response and in vivo glucose homeostasis. Mol Cell. 2001; 7:1165–1176. [PubMed: 11430820]

28. Cherkasova VA, Hinnebusch AG. Translational control by TOR and TAP42 through dephosphorylation of eIF2alpha kinase GCN2. Genes Dev. 2003; 17:859–872. [PubMed: 12654728]

29. Ma Y, Hendershot LM. The role of the unfolded protein response in tumour development: friend or foe? Nat Rev Cancer. 2004; 4:966–977. [PubMed: 15573118]

30. Cook JA, Gius D, Wink DA, Krishna MC, Russo A, Mitchell JB. Oxidative stress, redox, and the tumor microenvironment. Semin Radiat Oncol. 2004; 14:259–266. [PubMed: 15254869]

31. Yung HW, Korolchuk S, Tolkovsky AM, Charnock-Jones DS, Burton GJ. Endoplasmic reticulum stress exacerbates ischemia-reperfusion-induced apoptosis through attenuation of Akt protein synthesis in human choriocarcinoma cells. FASEB J. 2007; 21:872–884. [PubMed: 17167073]
32. Harding HP, Zhang Y, Zeng H, Novoa I, Lu PD, Calfon M, Sadri N, Yun C, Popko B, Paules R, Stojdl DF, Bell JC, Hettmann T, Leiden JM, Ron D. An integrated stress response regulates amino acid metabolism and resistance to oxidative stress. Mol Cell. 2003; 11:619–633. [PubMed: 12667446]
33. Back SH, Scheuner D, Han J, Song B, Ribick M, Wang J, Gildersleeve RD, Pennathur S, Kaufman RJ. Translation attenuation through eIF2alpha phosphorylation prevents oxidative stress and maintains the differentiated state in beta cells. Cell Metab. 2009; 10:13–26. [PubMed: 19583950]
34. Cullinan SB, Diehl JA. Coordination of ER and oxidative stress signaling: the PERK/Nrf2 signaling pathway. Int J Biochem Cell Biol. 2006; 38:317–332. [PubMed: 16290097]
35. Bi M, Naczki C, Koritzinsky M, Fels D, Blais J, Hu N, Harding H, Novoa I, Varia M, Raleigh J, Scheuner D, Kaufman RJ, Bell J, Ron D, Wouters BG, Koumenis C. ER stress-regulated translation increases tolerance to extreme hypoxia and promotes tumor growth. EMBO J. 2005; 24:3470–3481. [PubMed: 16148948]
36. Bobrovnikova-Marjon E, Grigoriadou C, Pytel D, Zhang F, Ye J, Koumenis C, Cavener D, Diehl JA. PERK promotes cancer cell proliferation and tumor growth by limiting oxidative DNA damage. Oncogene. 2010
37. Miyauchi H, Minamino T, Tateno K, Kunieda T, Toko H, Komuro I. Akt negatively regulates the in vitro lifespan of human endothelial cells via a p53/p21-dependent pathway. EMBO J. 2004; 23:212–220. [PubMed: 14713953]
38. Minamino T, Miyauchi H, Tateno K, Kunieda T, Komuro I. Akt-induced cellular senescence: implication for human disease. Cell Cycle. 2004; 3:449–451. [PubMed: 15004530]
39. Denoyelle C, Abou-Rjaily G, Bezrookove V, Verhaegen M, Johnson TM, Fullen DR, Pointer JN, Gruber SB, Su LD, Nikiforov MA, Kaufman RJ, Bastian BC, Soengas MS. Anti-oncogenic role of the endoplasmic reticulum differentially activated by mutations in the MAPK pathway. Nat Cell Biol. 2006; 8:1053–1063. [PubMed: 16964246]
40. Lin HK, Chen Z, Wang G, Nardella C, Lee SW, Chan CH, Yang WL, Wang J, Egia A, Nakayama KI, Cordon-Cardo C, Teruya-Feldstein J, Pandolfi PP. Skp2 targeting suppresses tumorigenesis by Arf-p53-independent cellular senescence. Nature. 2010; 464:374–379. [PubMed: 20237562]
41. Naidoo N. The endoplasmic reticulum stress response and aging. Rev Neurosci. 2009; 20:23–37. [PubMed: 19526732]
42. Kumar CC, Madison V. AKT crystal structure and AKT-specific inhibitors. Oncogene. 2005; 24:7493–7501. [PubMed: 16288296]
43. Krishnamoorthy J, Mounir Z, Raven JF, Koromilas AE. The eIF2alpha kinases inhibit vesicular stomatitis virus replication independently of eIF2alpha phosphorylation. Cell Cycle. 2008; 7:2346–2351. [PubMed: 18677106]
44. Kazemi S, Mounir Z, Baltzis D, Raven JF, Wang S, Krishnamoorthy JL, Pluquet O, Pelletier J, Koromilas AE. A novel function of eIF2alpha kinases as inducers of the phosphoinositide-3 kinase signaling pathway. Mol Biol Cell. 2007; 18:3635–3644. [PubMed: 17596516]
45. Lizcano JM, Alrubaie S, Kieloch A, Deak M, Leevers SJ, Alessi DR. Insulin-induced Drosophila S6 kinase activation requires phosphoinositide 3-kinase and protein kinase B. Biochem J. 2003; 374:297–306. [PubMed: 12841848]

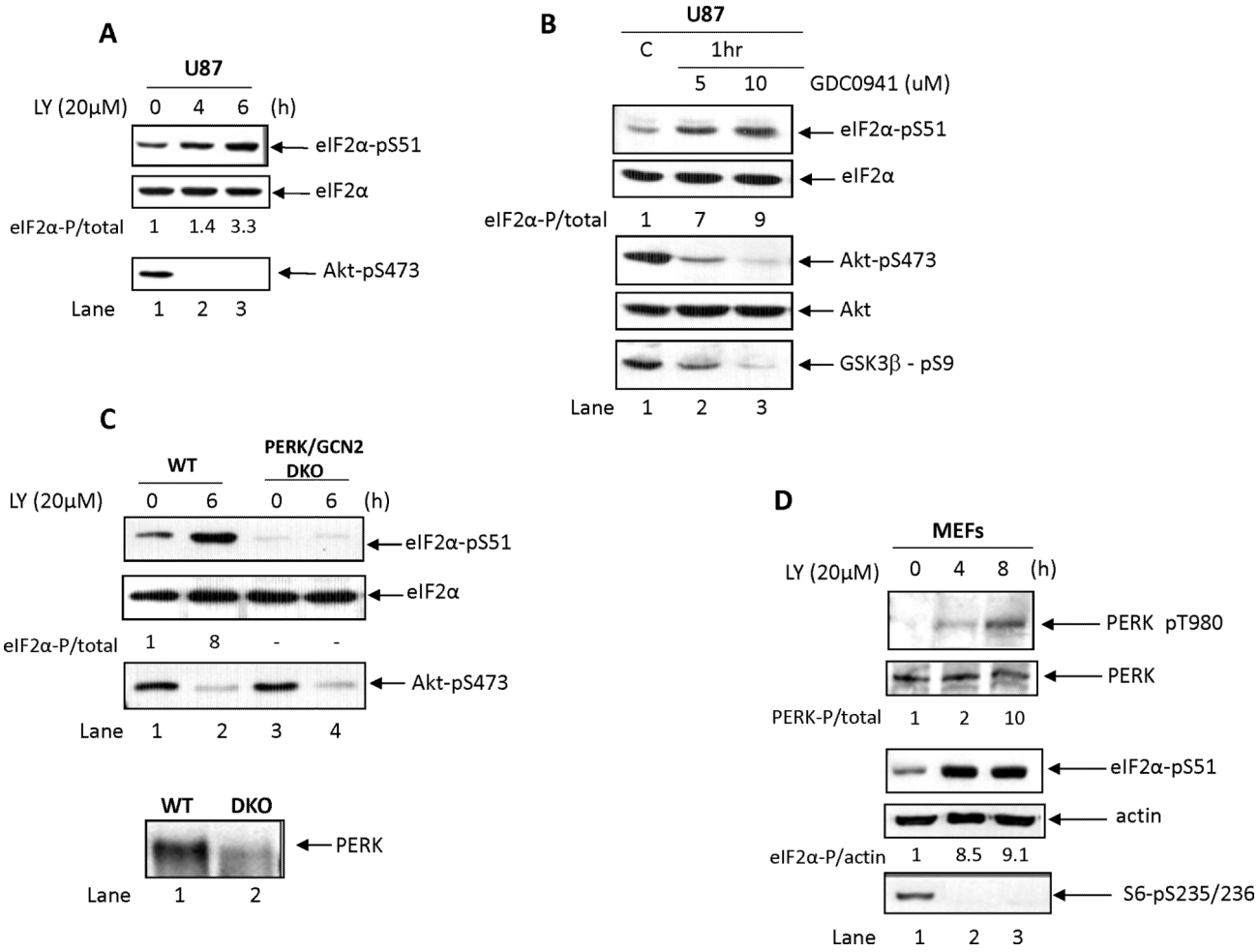

Figure 1. Induction of eIF2αP by PI3K inhibition requires PERK and GCN2

(A, B) Human glioblastoma U87 cells were left untreated (**A–B,** lane 1) or treated with 20μM LY294002 (**A,** lanes 2–3) or with 5μM and 10μM GDC-0941 (**B,** lanes 2–3) for the indicated hours (h). (**C**) Isogenic WT or PERK$^{-/-}$GCN2$^{-/-}$ (double knockout; DKO) MEFs were left untreated (**C,** lanes 1, 3) or treated with 20 μM LY294002 (**C**, lanes 2, 4) for 6 h. (**D**) Immortalized WT MEFs were left untreated (lane 1) or treated with 20μM LY294002 for the indicated hours (h). (**A–D**) Protein extracts (50 μg) were immunoblotted for the indicated proteins. The ratio of eIF2αP to total eIF2α or actin and phosphorylated PERK to total PERK for each lane is indicated. Panels A to D are representative of three independent experiments.

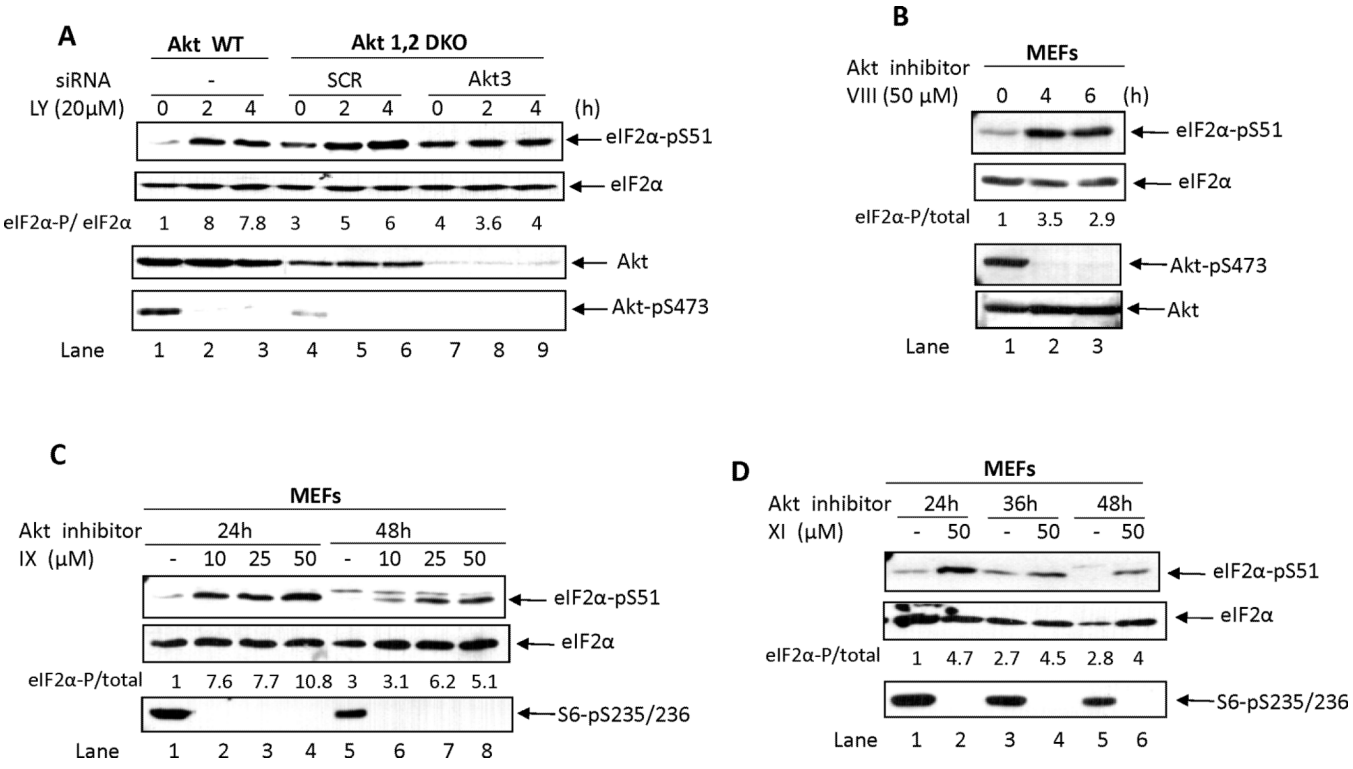

Figure 2. Akt inactivation causes the induction of eIF2αP

(A) Akt wild-type (WT) cells were left untreated (lane 1) or treated with 20 μM LY294002 (lanes 2, 3) for the indicated hours (h). $Akt1^{-/-}Akt2^{-/-}$ (double knockout; DKO) MEFs were treated with either scrambled control siRNA (lanes 4–6) or siRNA against Akt3 (lanes 7–9) in the absence (lanes 4, 7) or presence of 20 μM LY294002 (lanes 5, 6, 8, 9) for the indicated hours (h). (**B–D**) Immortalized wild-type MEFs were treated with the indicated concentrations of Akt inhibitor VIII (**C**), IX (**D**) or XI (**E**) for different times (h). (**A–D**) Protein extracts (50 μg) were immunoblotted for the indicated proteins. The ratio of eIF2αP to either total eIF2α or actin for each lane is indicated. Panels A to D are representative of three independent experiments.

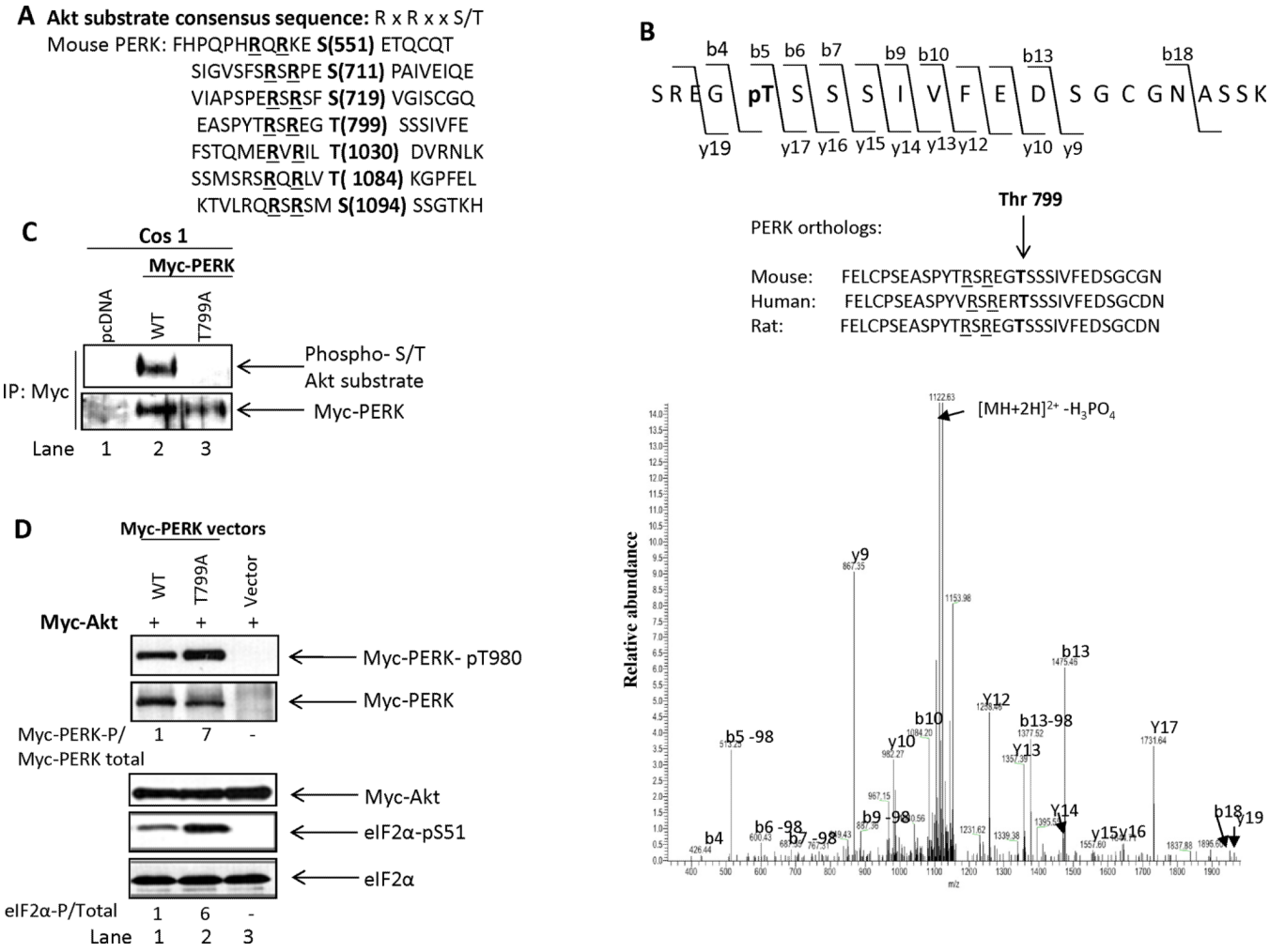

Figure 3. Akt inactivates PERK by phosphorylation at threonine 799

(**A**) Sequence alignment of putative Akt phosphorylation sites in mouse PERK. **(B)** MS2 spectrum of SREGpTSSSIVFEDSGCGNASSK phosphopeptide of mouse PERK phosphorylated by Akt1 subjected to in-gel digestion with trypsin. The analysis was performed on a LTQ linear ion trap mass spectrometer. MS/MS spectra were assigned with MASCOT as described in Materials and Methods. Scaffold was used to filter MS/MS based identification and annotate MS/MS spectra. The spectrum shows a peptide, which contains the phosphothreonine 799 residue identified by the analysis of the peptide's y and b fragments. An intense neutral loss of phosphoric acid (−98) was observed from the precursor ion (peaks at 1122.63). Alignment of the amino acid sequence surrounding the T799 phosphorylation site indicates its conservation in mouse, human and rat PERK orthologs. (**C**) Cos-1 cells (5×10^5) were transfected with 5 μg of pcDNA-empty vector DNA (lane 1) or 5 μg of pcDNA-vector containing either Myc-tagged mouse PERK wild type (WT) cDNA (lane 2) or Myc-tagged mouse PERK T799A cDNA (lane 3). Forty-eight hours after transfection, protein extracts (500 μg) were subjected to immunoprecipitation with anti-Myc antibody followed by immunoblotting with anti-phospho S/T Akt substrate antibody (top panel) or anti-Myc antibody (bottom panel). (**D**) Cos1 cells (5×10^5) were transfected with 2.5 μg of pcDNA vector containing Myc-Akt1 cDNA (lanes 1–3) and 2.5 μg of pcDNA-vector containing Myc-PERK WT cDNA (lane 1), Myc-PERK T799A cDNA (lane 2) or pcDNA vector alone (lane 3). Forty-eight hours after transfection, protein extracts (50 μg)

were immunoblotted for the indicated proteins. The ratio of phosphorylated Myc-PERK to total Myc-PERK as well as eIF2αP to total eIF2α for each lane is indicated. Panels C and D are representative of three independent experiments.

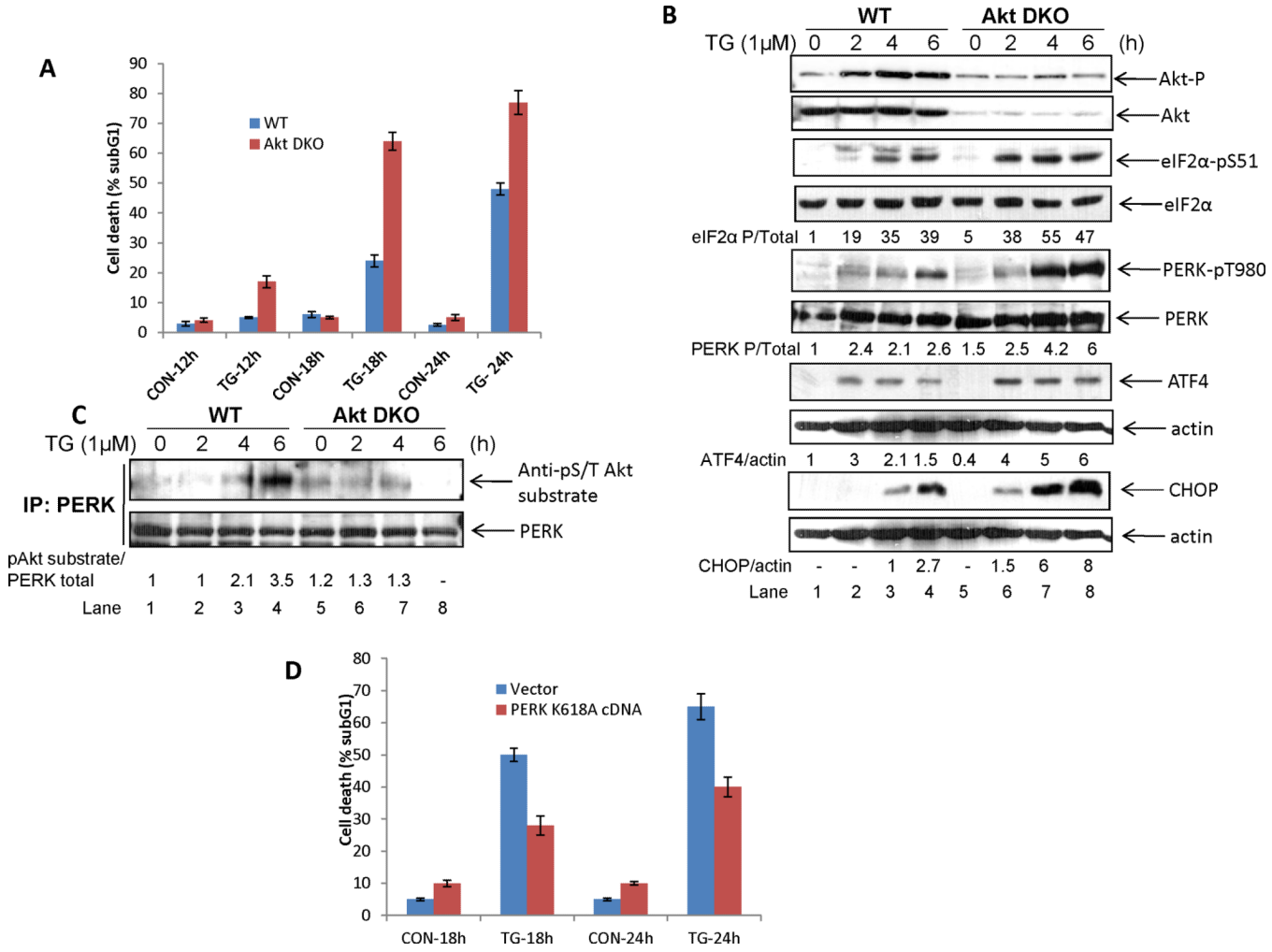

Figure 4. PERK counteracts the pro-survival properties of Akt in ER-stressed cells

(A) Isogenic WT MEFs and Akt DKO MEFs were treated with 1 μM thapsigargin (TG) for the indicated hours (h). Cell death (% subG1) was determined by propidium iodide staining and flow cytometry analysis. Histograms show quantification of results from three independent experiments; error bars indicate SD, n=3. The group difference was tested by ANOVA (P<0.0004 for comparison). (**B, C**) WT and Akt DKO MEFs were treated with 1 μM TG for the indicated hours (h). (**B**) Protein extracts (50 μg) were immunoblotted for the indicated proteins. The ratio of eIF2αP to total eIF2α, T980 phosphorylated PERK to total PERK as well as the ratio of ATF4 or CHOP to actin for each lane is indicated. (**C**) Protein extracts (500 μg) were subjected to immunoprecipitation with anti-PERK antibody followed by immunoblotting with anti-phospho S/T Akt substrate antibody (top panel) or PERK antibody (bottom panel). The ratio of phosphorylated PERK to total PERK for each lane is indicated. (**D**) Akt DKO MEFs were transfected with 10 μg of pcDNA vector alone or 10 μg pcDNA vector bearing Myc-PERK K618A cDNA in the presence of 5 μg vector containing the GFP cDNA. Cells were treated with TG for 18 and/or 24 h and stained with Hoechst 33342. Cell death (% subG1) was assessed in cells expressing GFP by cell sorting and flow cytometry analyses. Histograms show quantification of results from three independent experiments; error bars indicate SD, n=3. The group difference was tested by ANOVA (P<0.0006). Panels B and C are representative of three independent experiments.

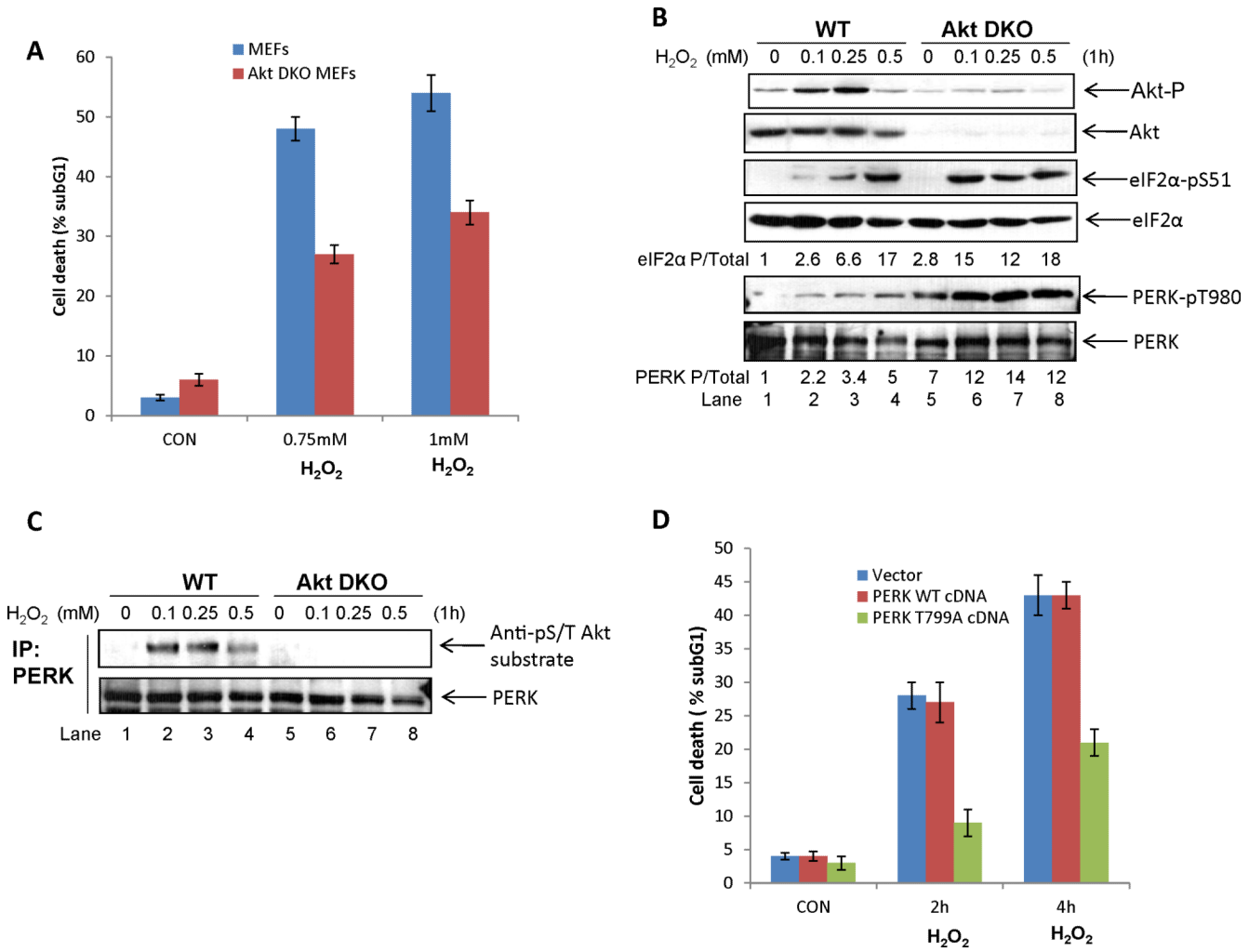

Figure 5. PERK antagonizes the pro-apoptotic function of Akt in response to oxidative stress

(A) Isogenic WT MEFs and Akt DKO MEFs were treated with 0.75 mM or 1 mM H2O2 for 1 hour. Cell death (% subG1) was determined by propidium iodide staining and flow cytometry analysis. Histograms show quantification of results from three independent experiments; error bars indicate SD, n=3. The group difference was tested by ANOVA (*P*<0.0002 for comparison). (**B, C**) WT and Akt DKO MEFs were treated with increased concentrations of H2O2 for 1 h. (**B**) Protein extracts (50 μg) were immunoblotted for the indicated proteins. The ratio of eIF2αP to total eIF2α and T980 phosphorylated PERK to total PERK for each lane is indicated. (**C**) Protein extracts (500 μg) were subjected to immunoprecipitation with anti-PERK antibody followed by immunoblotting with anti-phospho S/T Akt substrate antibody (top panel) or PERK antibody (bottom panel). (**D**) PERK$^{-/-}$ MEFs were transfected with 10 μg of pcDNA vector alone or 10 μg pcDNA vector bearing either Myc-PERK WT cDNA or Myc-PERKT799A cDNA in the presence of 5 μg vector containing the GFP cDNA. Cells were treated with H2O2 (0.5mM) for 1 h and stained with Hoechst 33342. Cell death (% subG1) was assessed in cells expressing GFP by cell sorting and flow cytometry analyses. Histograms show quantification of results from three independent experiments; error bars indicate SD, n=3. The group difference was tested by ANOVA (*P*<0.0002 for comparison). Panels B and C are representative of three independent experiments.

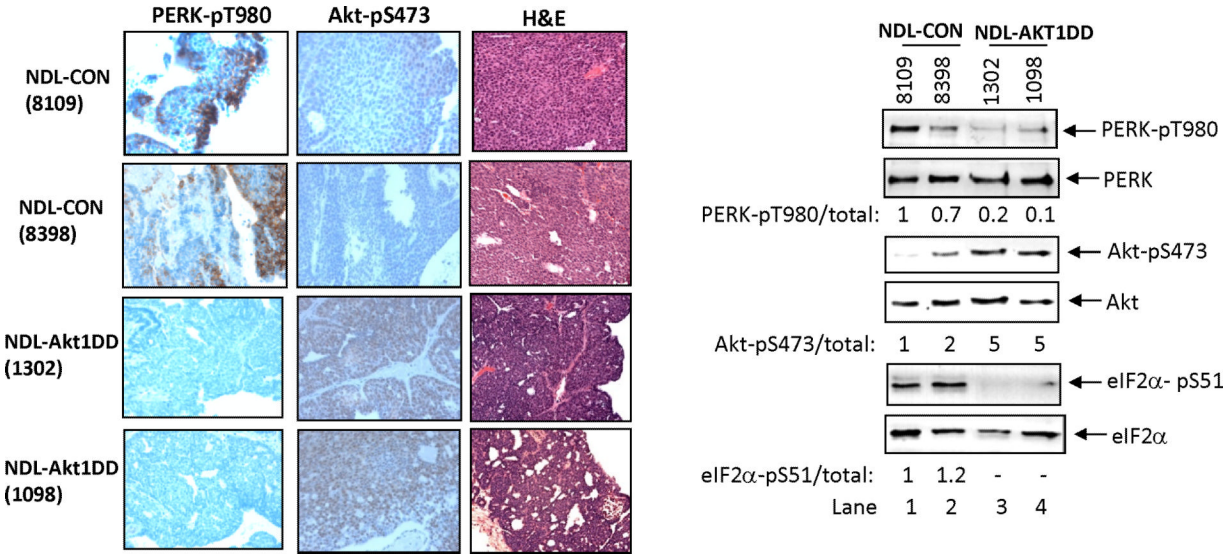

Figure 6. Akt downregulates PERK activity and eIF2αP in mouse mammary gland tumors *in vivo*

Mammary tumors from transgenic mice expressing either NDL 2–5 alone (NDL-CON; #8109, #8398) or NDL 2–5 together with hyperactive Akt1-DD (NDL-Akt1DD; #1098, #1302) subjected to IHC analysis for PERK phosphorylated at T980 (PERK-pT980), Akt phsophorylated at S473 (Akt-pS473) as well as hematoxylin and eosin (H&E) staining (left panel). Lysates of mammary tumors from NDL-CON or NDL-Akt1DD mice were immunoblotted for the indicated proteins. The ratio of phosphorylated PERK to total PERK, phosphorylated Akt to total Akt and eIF2αP to total eIF2α for each lane is indicated (right panel).

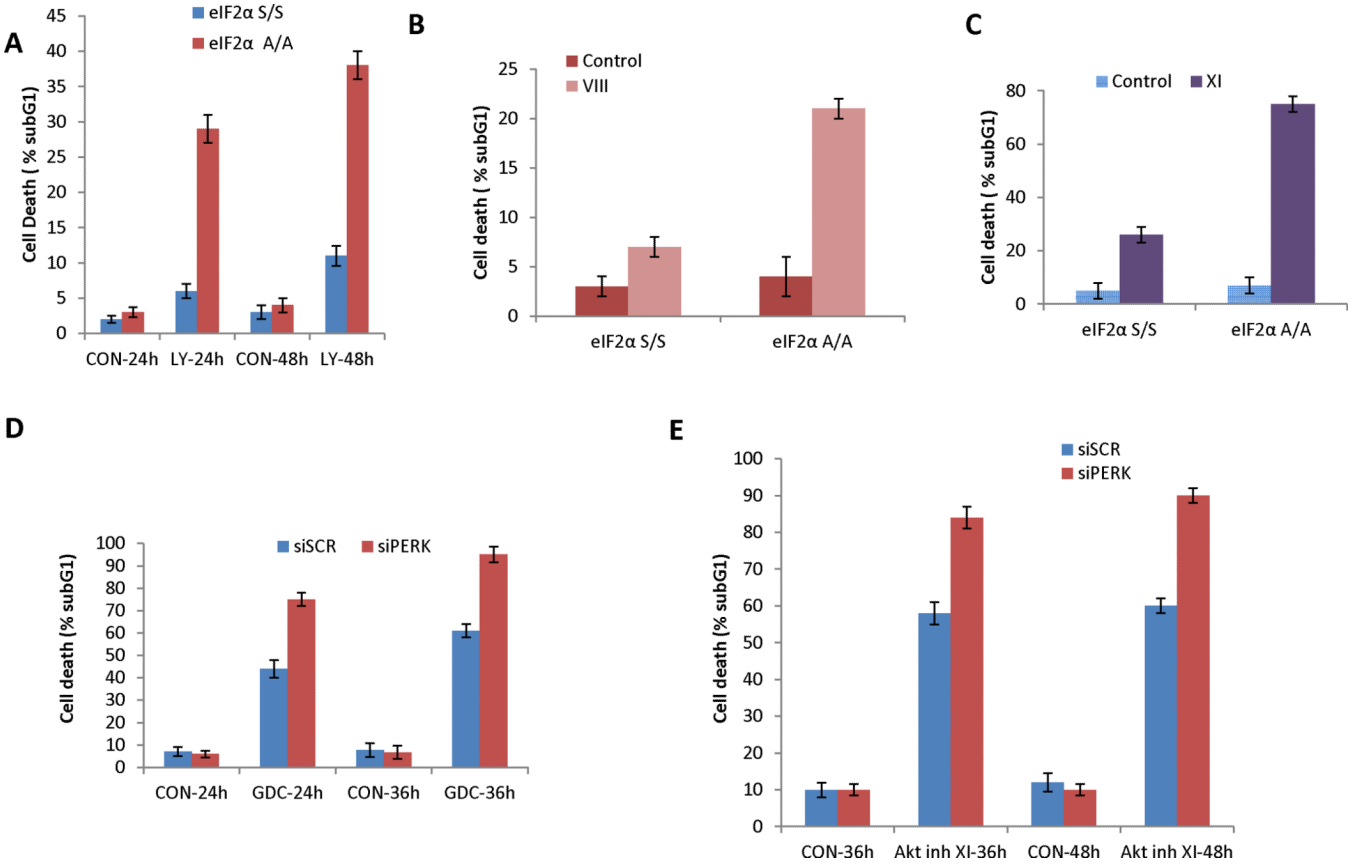

Figure 7. The PERK-eIF2αP arm promotes cell survival and reduces the efficacy of anti-tumor treatment with inhibitors of PI3K and Akt

Isogenic eIF2α S/S and eIF2α A/A MEFs were treated with 20 μM LY294002 for 24 or 48 h (**A**), 50 μM Akt inhibitor VIII for 12h (**B**), or 50 μM Akt inhibitor XI for 48 h (**C**). HT1080 cells were treated with either scrambled control siRNA or siRNA against PERK in the absence or presence of either 10 μM GDC-0941 (**D**) or 50 μM Akt inhibitor XI (**E**) for the indicated hours (h). Cell death (% subG1) (**A–E**) was assessed by propidium iodide staining and flow cytometry analysis. (**A**) Histograms show quantification of results from seven independent experiments; error bars indicate SD, n=7. The group difference was tested by ANOVA ($P<0.0004$ for comparison). (**B–E**) Histograms show quantification of results from three independent experiments; error bars indicate SD, n=3. The group difference was tested by ANOVA (**B:** $P<0.002$; **C:** $P<0.0001$; **D:** $P<0.001$; **E:** $P<0.001$ for comparison).